Effect of random impurities on transport characteristics of nano-scale MOSFET

Gennady Mil'nikov*, Nobuya Mori
and Yoshinari Kamakura
Department of Electrical, Electronic and
Information Engineering
Osaka University, Suita, Japan
Email: gena@e3.eei.eng.osaka-u.jp

Tatsuya Ezaki
Graduate School of Engineering
Hiroshima University
Hiroshima, Japan

***Abstract*—Recently, we have proposed a new method for device simulations which allows for splitting the device area into a set of independent elements and computing all the physical observables in the form of local spectral representation. The shape of the device elements and their internal coordinate representation are arbitrary which offers a natural way to treat singular dopant charge distribution by choosing appropriate device fragmentation scheme. We have applied our method to study the impact of an attractive ion in intrinsic Si channel to the MOSFET transport characteristics. We have observed an intrinsic bistability in biased MOSFETs related with two possible ion charge screening mechanisms.**

I. Introduction

Recent progress in semiconductor industry has been largely stimulated by decreasing size of CMOS (complementary metal-oxide semiconductor) elements. Present-day technology makes it possible to fabricate CMOS based field-effect transistors with channel length of 45 nm, and MOSFET with much shorter channel 10 nm are predicted to become mass-produced within few technology generations. Scaling towards miniaturization has led to the development of a variety of novel devices such as double gate transistors, carbon nanotubes and gate-all-around (GAA) MOSFET nanowires. One of the major sources of variability of these structures is random discrete dopants distribution. As the size of CMOS shrinks, variation in dopant position leads to measurable difference in macroscopic parameters, such as drive current and leakage. Dopants could also be used as a functional part of device. Electron tunneling through isolated dopants has been observed in GaAs/AlAs heterostructures [1] and spectroscopy of a single dopant in nanowire has been reported recently [2]. Strong influence on dielectric environment on dopant scattering and electron mobility in semiconductor nanostructures has also been predicted [3]. Variability in the dopants position is inherently three-dimensional problem and development of effective tools for modeling such effects is still imperative. Application of the Non Equilibrium Green's function (NEGF) formalism with ordinary real space grid representation is hampered by increasing number of the mesh points and huge size of the device Hamiltonian. Accurate numerical study of the attractive ions is especially difficult. In nanoscale regime, the device electrostatics is strongly affected by the screening charge, which in turn is sensitive to the position of the resonant levels in screened attractive Coulomb potential. Moreover, interaction of the resonant states at different Coulomb centers depends on the quantum phases, which implies that the wave function needs to be computed accurately at the Coulomb centers. In this work we show that our method gives such accurate solutions with minor extra computational efforts. We perform self-consistent three dimensional quantum transport simulations for the MOSFETs with single attractive ion in the intrinsic Si channel and study its impact on the device transport characteristics.

II. R-matrix theory and device growth algorithm

In this section we outline the R-matrix theory of quantum transport [4] and summarize our computational procedure. We shall restrict our consideration to the simplest case of the electronic wave function $\Psi(\mathbf{r})$ in parabolic conduction band and put $m^* = \hbar = 1$. In order to avoid the real space grid representation, we construct $\Psi(\mathbf{r})$ as a linear combination of real-valued basis functions $\{\Phi_n(\mathbf{r})\}$. Then, the one-particle Hamiltonian

$$\mathbf{H} = -\frac{1}{2}\nabla^2 - e\varphi(\mathbf{r}) \tag{1}$$

is completely defined by the corresponding matrix elements $H_{nm} = (\Phi_n|\mathbf{H}|\Phi_m)$. Importantly, the basis functions $\Phi_n(\mathbf{r})$ must be free from any kind of homogeneous boundary conditions in order to describe a non-zero electric current. As a result, the matrix element of the kinetic energy contains a non-symmetric surface contribution and the Hamiltonian $\mathbf{H}$ is not Hermitian. We introduce the effective $close$ system Hamiltonian $\widetilde{\mathbf{H}}$ with symmetrized kinetic energy

$$\begin{aligned}\widetilde{H}_{nm} &= \int d\mathbf{r}\left[\frac{1}{2}\nabla\Phi_n(\mathbf{r})\nabla\Phi_m(\mathbf{r})\right. \\ &- \left.\Phi_n(\mathbf{r})e\varphi(\mathbf{r})\Phi_m(\mathbf{r})\right]\end{aligned} \tag{2}$$

and use its eigenvalues

$$\widetilde{\mathbf{H}}\Phi_n = E_n\Phi_n. \tag{3}$$

978-1-4244-1753-7/08/$25.00 ©2008 IEEE

as the basis functions. Then an arbitrary wave function is represented in the form [4]

$$\Psi(\mathbf{r}) = \sum_n \frac{\Phi_n(\mathbf{r})}{2\,(E_n - \varepsilon)} \sum_\nu \langle \Phi_n|\nu\rangle I_\nu, \tag{4}$$

where $\langle ...|...\rangle$ stands for integration over the device surface, $\{|\nu\rangle\}$ is a supplementary surface basis and $I_\nu \equiv \langle \nu|\frac{d\Psi}{d\mathbf{n}}\rangle$ play a role of unknown parameters. We introduce the R-matrix $R_{\nu\mu}$ which, by definition, gives a linear relation between the wave function and its normal derivative I_ν on the device surface:

$$\langle \nu|\Psi\rangle = \sum_\mu R_{\nu\mu} I_\mu, . \tag{5}$$

The spectral representation for the R-matrix follows from Eq.(4):

$$R_{\nu\mu} = \sum_n \frac{\langle \nu|\Phi_n\rangle\langle\Phi_n|\mu\rangle}{2(E_n - \varepsilon)}. \tag{6}$$

Eqs. (4),(5) and (6) are the working equations of the R-matrix theory. Once the R-matrix is found, the scattering boundary conditions simultaneously generate transmittion coefficients for all the leads and the boundary parameters I_ν at the corresponding contacts. Thus, one can compute the electric current in the Landauer formula[5] and the wave function in Eq.(4), i.e. the carrier density.

The basis $\{\Phi_n\}$ is generally to be computed by diagonalizing the Hamiltonian matrix Eq. (2) in terms of appropriate primary basis. In three dimensional domain with singular electrostatic potential solving the global spectral problem Eq. (3) is not possible. On the other hand, the R-matrix Eq.(5) can be defined at any surface inside the device area and it does not depend on the basis representation. The device growth algorithm[4] enables the R-matrix to be propagated through the device area and eliminates the huge eigenvalue problem. We split the device area into a set of elements where the wave function is well represented by small primary basis sets. Then, the Hamiltonian matrix Eq.(2) is computed separately in each element and small independent spectral problems are easily solved. We start with an arbitrary element and grow the device by adding all the other elements one by one. After adding a new element, the device boundary changes and a part of the previous boundary is removed. Given the surface basis $\{|\nu\rangle\}$ at the removed boundary segment, we require the continuity of $\langle\nu|\Psi\rangle$ which gives algebraic recipe for the R-matrix propagation[4]. Computing the R-matrix at each step only requires inversion of a boundary matrix of small size of $\{|\nu\rangle\}$. The R-matrix propagation also generates a set of successive relations which express $\{I_\nu\}$ at each boundary segment in terms of $\{I_\nu\}$ on the surface of the growing device after removing this segment. Eq. (6) in the first element gives initial conditions for the device growth. Adding the last element completes the device and gives the R-matrix and the boundary parameters I_ν at the contacts which suffice to compute the electric current in all the leads. In turn, successive boundary relations generate I_{nu} at all previously removed internal boundary segments and give local basis representation

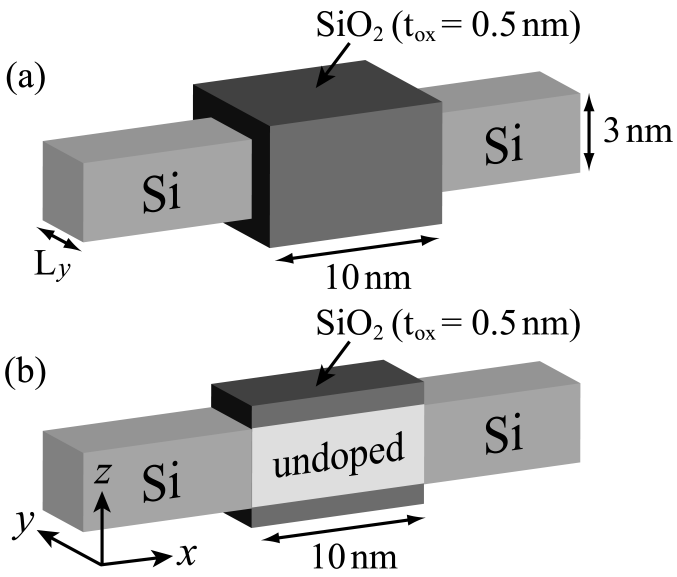

Fig. 1. GAA and double gate MOSFET used in the simulations.

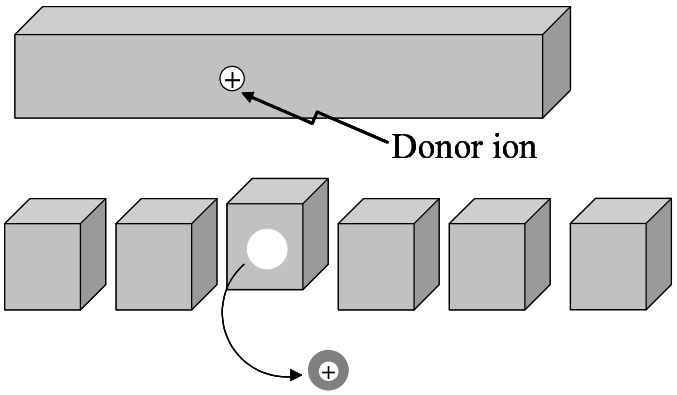

Fig. 2. Fragmentation scheme for a device with Coulomb singularity.

for the carrier density in each device element. Thus, using the device growth algorithm, we avoid huge calculations and the computation time scales linearly with the device volume [4].

III. Electrostatic potential with Coulomb singularities

Apart from its numerical efficiency, the method offers a natural way to study effect of random dopants by adjusting the device fragmentation scheme. In this work, we calculate a ballistic transport at $T = 300K$ in the GAA and double gate Si MOSFET (Fig. 1). in the effective mass approximation with $m^* = 0.26$, $\epsilon_{\rm Si} = 11.9$, $\epsilon_{\rm SiO_2} = 3.8$, dopant concentration in the source/drain region of $10^{20}\,{\rm cm}^{-3}$, the length in y-direction $L_y = 2,3$ nm and applied bias $V_{\rm SD} = 0.1\,{\rm V}$. We take the direction from source to drain as the positive x-direction. We place a single positive charge in the gate area and compute the drain current as a function of the gate voltage V_{GATE} at different positions of the donor.

The device elements are introduced by first dividing the the semiconductor area along the x-direction and than separating

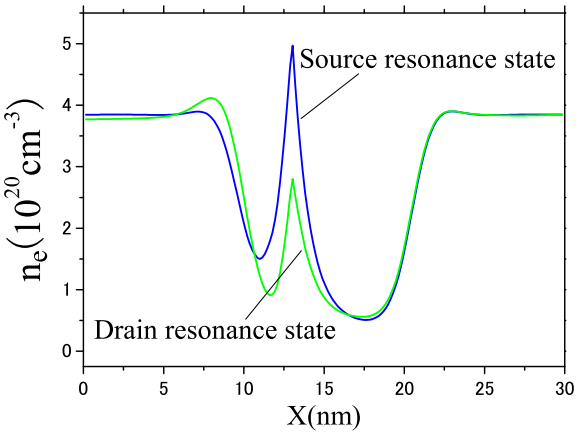

Fig. 3. Carrier density along the current direction in the middle of the Si channel. The donor is located in the middle of (y, z)-plane at x_d=13 nm. The green and blue curves correspond to two possible screening mechanisms in Fig. 7.

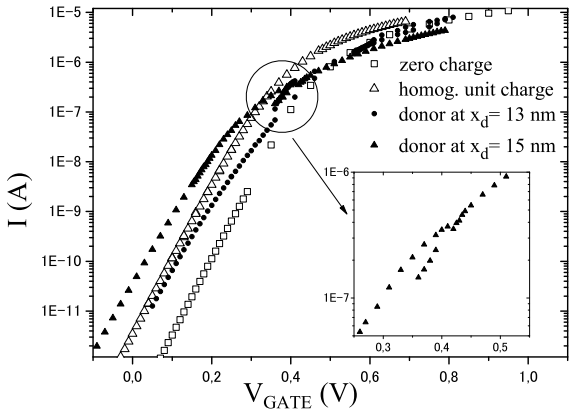

Fig. 4. I-V characteristics for the MOEFET on Fig. 1b. Four curves correspond to the intrinsic channel (open squares), homogeneous positive unit charge in the channel (open triangles), and positive ion at x_d=13 nm (solid circles) and x_d=15 nm (solid triangle). Inset shows bistability of the electronic state for x_d=15 nm.

out the spherical element centered at the donor position (Fig. 2). Thus, there are three types of the device elements: rectangular, rectangular with spherical hole and spherical. In the former two, the primary basis is constructed by the SDT method in terms of DVR Jacobi polynomials [4]. In the latter we use spherical coordinates (ρ, θ, ϕ) and take as a basis the direct product of spherical harmonics $Y_{lm}(\theta, \phi)$ and Legender polynomials $P_n(\rho)$. $Y_{lm}(\theta, \phi)$ are also used as the basis $\{|\nu\rangle\}$ at the surface of spherical element. Using spherical coordinates eliminates the Coulomb singularity and the wave function at the donor is computed easily.

In our method, smoothness of the carrier density at the internal boundaries between the device elements provides a universal criterium for numerical completeness of the local spectral expansions and the surface bases. Fig. 3 shows a typical behaviour of the density along the current direction in the middle of Si body. The peaks in the figure are located exactly at the donor position.

The curve on Fig. 3 is composed from separate pieces computed in all the device elements but the global solution is clearly smooth, which guarantees that implemented bases are large enough. We confirmed at least three significant digits of accuracy by changing the radius of the spherical element from 0.25 to 0.8 nm and number of spherical harmonics from 16 ($l = 3$) to 36 ($l = 5$). Typical basis size in these calculations is $\sim 50 - 80$ for the rectangular elements and ~ 100 for the spherical element. From the numerical viewpoint, the existence of the donor entails additional spherical element which only causes ~ 20 % increase in computer time compared to smooth charge distribution. The Poisson equation with point charge singularity was solved by the method of [6]

IV. Simulation results

In Fig. 4 we compare the I-V characteristics for the double gate MOSFET with zero positive charge in the channel, homogeneously distributed unit charge and with the positive ion located in the middle of y, z plane at $x_d = 13$ nm and 15 nm. In the substhreshold region, the drain current strongly depends on the donor position which cannot be mimicked by smooth charge distribution. The strongest effect is for the donor in the middle of the Si body, and this tendency is observed in our calculations for different L_y in both double Gate and GAA MOSFETs.

We have also found two branches in the IV characteristics which indicates an intrinsic instability of the non-equlibrium electronic state of the device. The inset on Fig. 4 shows an example of this bistability in double gate MOSFET with the donor at $x_d = 15$ nm. On Fig. 5 we present comprehensive data for GAA MOSFET with voltage resolution $\Delta V_{GATE} = 0.002V$. For $x_d = 15$ nm, two stable states are found within voltage interval ~ 0.05 V. When the donor is shifted in the source direction, the bistability region increases up to ~ 0.2 nm.

The origin of the instinsic bistabilily can be seen from Figs. 6 and 7 which show the transmition function T(E) and energy resolution of the screening charge in the gate area for two electronic states in GAA with $x_d = 13$ nm at $V_{GATE} = 0.4$ V. The blue (green) curves on these figures correspond to the upper (lower) branch in Fig. 5. The carrier density for these states is shown in Fig. 3. We observe the resonant contribution to the drain current (blue curve) and the corresponding peak in the screening charge at energies above the bottom of the lowest conduction subband in the source region (located at ~ 0 eV). In this state, the ion is mostly screened by trapped source electrons. On the contrary, the narrow green resonance is below the threshould for the source electrons. The ion is mostly screened by the drain electrons which do not contribute to the drain current. The

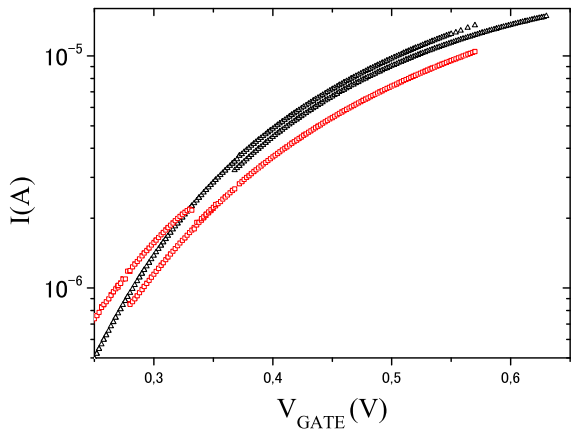

Fig. 5. Bistability in the IV characteristics of the GAA MOSFET on Fig.1a. The donor is located at $x_d = 15$ nm (red) and $x_d = 13$ nm (black).

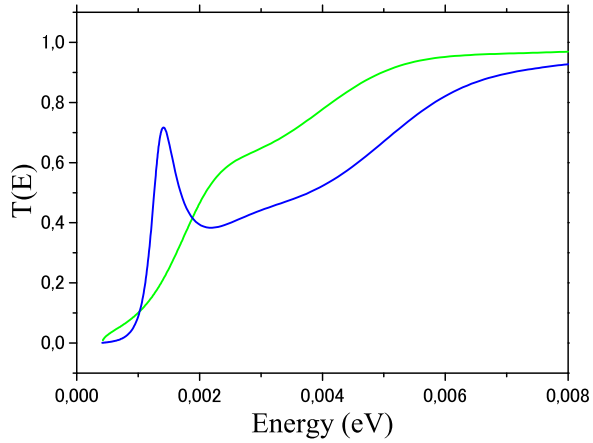

Fig. 6. Transmission function T(E) for two screening mechanisms in Fig. 7.

total screening charge trapped by the ion in the blue state ("source resonance") exceeds the one in the green state ("drain resonance") (see Fig. 3), which in turn causes the shift in the resonant energy due to the feedback effect. A comprehensive analysis of this peculiar behaviour is beyond the scope of this paper and will be given elsewhere.

ACKNOWLEDGMENT

This work was supported by Industrial Technology Research Grant Program in 2005 from New Energy and Industrial Technology Development Organization (NEDO) of Japan.

REFERENCES

[1] M. W. Dellow et al., *Resonant tunneling through the bound states of a single donor arom in a quantum well* , Phys. Rev. Lett, vol. 68, pp.1754-1757, 1992.

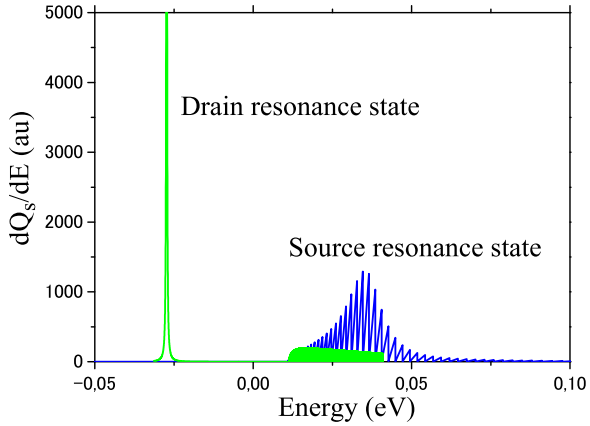

Fig. 7. Spectrum of the screening charge in the gate area for two states in Fig. 3. Blue (green) state corresponds to screening the ion charge by source (drain) electrons.

[2] H. Sellier et al., *Transport Spectroscopy of a Single Dopant in a Gated Silicon Nanowire*, Phys. Rev. Lett., vol. 97, pp.206805-206808, 2006

[3] D. Jena and A. Konar, *Enhancement of Carrier Mobility in Semiconductor Nanstructures by Dielectric Engineering*, Phys. Rev. Lett., vol. 98, pp. 136805-136808, 2007.

[4] G. Mil'nikov, N. Mori, Y. Kamakura, and T. Ezaki, *R-matrix theory of quantum transport and recursive propagation method for device simulations*, J. Appl. Phys., in press.

[5] S. Datta, *Electronic Transport in Mesoscopic Systems*, Cambridge, University Press, 1995.

[6] G. Mil'nikov, N. Mori, Y. Kamakura, and T. Ezaki, *Solution of the Poisson equation with coulomb singularities*, Jpn. J. Appl. Phys., in press.